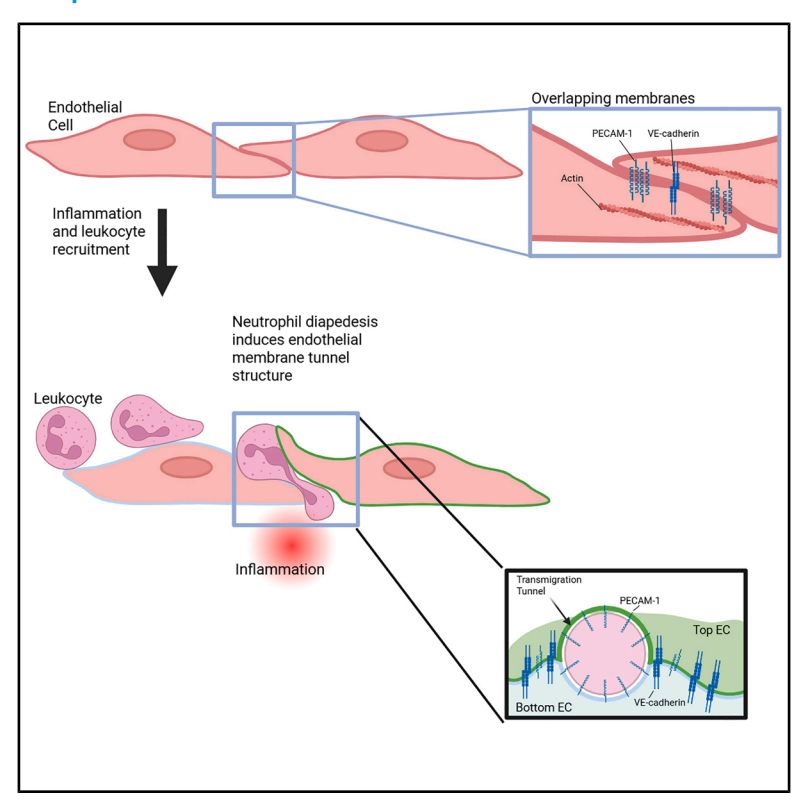
Leukocytes use endothelial membrane tunnels to extravasate the vasculature

Graphical abstract



Authors

Werner J. van der Meer, Abraham C. I. van Steen, Eike Mahlandt, ..., Sussan Nourshargh, Joachim Goedhart, Jaap D. van Buul

Correspondence

j.d.vanbuul@amsterdamumc.nl

In brief

During paracellular transmigration, neutrophils exit the vasculature not through simple endothelial retraction but via dynamic membrane tunnels formed by overlapping endothelial cells. Using high-resolution live imaging, the authors et al. reveal that neutrophils actively remodel endothelial membranes to create 3D exit tunnels.

Highlights

- Endothelial cells overlap at junction regions beyond VEcadherin
- Leukocytes prefer endothelial membrane overlaps to extravasate
- PECAM-1 serves as a marker for EC overlaps







Article

Leukocytes use endothelial membrane tunnels to extravasate the vasculature

Werner J. van der Meer, ^{1,2,10} Abraham C.I. van Steen, ^{2,10} Eike Mahlandt, ^{1,3} Loïc Rolas, ^{4,5} Haitao Wang, ^{4,5} Janine J.G. Arts, ² Lanette Kempers, ² Max L.B. Grönloh, ^{1,2} Rianne M. Schoon, ¹ Amber Driessen, ² Jos van Rijssel, ² Ingeborg Klaassen, ⁶ Reinier O. Schlingemann, ⁶ Yosif Manavski, ⁷ Mark Hoogenboezem, ⁸ Reinier A. Boon, ⁷ Satya Khuon, ⁹ Eric Wait, ⁹ John Heddleston, ⁹ Teng-Leong Chew, ⁹ Martijn A. Nolte, ⁸ Sussan Nourshargh, ^{4,5} Joachim Goedhart, ³ and Jaap D. van Buul^{1,2,3,11,*}

¹Vascular Cell Biology Lab, Department of Medical Biochemistry, Amsterdam UMC, University of Amsterdam, Amsterdam, the Netherlands ²Molecular Cell Biology Lab, Department of Molecular Hematology, Sanquin Research, and Landsteiner Laboratory, Amsterdam, the Netherlands

³Leeuwenhoek Centre for Advanced Microscopy, Molecular Cytology Section, Swammerdam Institute for Life Sciences, University of Amsterdam, Amsterdam, the Netherlands

⁴Centre for Microvascular Research, William Harvey Research Institute, Faculty of Medicine and Dentistry, Queen Mary University of London, London, UK

⁵Centre for Inflammation and Therapeutic Innovation, Queen Mary University of London, London, UK

⁶Department of Ophthalmology at Amsterdam UMC, University of Amsterdam location, Department of Ophthalmology, University of Lausanne, Jules-Gonin Eye Hospital, Fondation Asile des Aveugles, Lausanne, Switzerland

⁷The Institute for Cardiovascular Regeneration, Center of Molecular Medicine, Goethe University, Frankfurt, Germany

⁸Core Facility at Department Molecular Hematology, Sanquin Research and Landsteiner Laboratory, Amsterdam, the Netherlands

⁹Advanced Imaging Center at Janelia Research Campus, Howard Hughes Medical Institute, Ashburn, VA, USA

¹⁰These authors contributed equally

¹¹Lead contact

*Correspondence: j.d.vanbuul@amsterdamumc.nl https://doi.org/10.1016/j.celrep.2025.116242

SUMMARY

Upon inflammation, leukocytes extravasate through endothelial cells. When they extravasate, it is generally accepted that neighboring endothelial cells disconnect. Careful examination of endothelial junctions showed a partial membrane overlap beyond VE-cadherin distribution. These overlaps are regulated by actin polymerization and, although marked by, do not require PECAM-1, nor VE-cadherin. Neutrophils prefer wider membrane overlaps as exit sites. Detailed 3D analysis of neutrophil transmigration in real time at high spatiotemporal resolution revealed that overlapping endothelial membranes form a tunnel during neutrophil transmigration. These tunnels are formed by the neutrophil lifting the membrane of the upper endothelial cell while indenting and crawling over the membrane of the underlying endothelial cell. Our work shows that endothelial cells do not simply retract upon the passage of neutrophils but provide membrane tunnels, allowing neutrophils to extravasate. This discovery defines the 3D multicellular architecture in which the paracellular transmigration of neutrophils occurs.

INTRODUCTION

The immune system protects our body from bacteria, viruses, parasites, and injury. To reach the site of infection, immune cells extravasate the circulation and penetrate the vessel wall in a process known as leukocyte transendothelial migration (TEM). This process is understood to occur in at least three distinguished steps: rolling, adhesion, and diapedesis. The latter step can occur in two ways: paracellular, i.e., through cell-cell junctions, or transcellular, i.e., through the endothelial cell (EC) body. The TEM model was first proposed by Butcher and further defined by Springer. Although many studies have added to our understanding, the principles of the "multistep paradigm" model still stand. One of the dogmas is that during the final dia-

pedesis step, when the leukocytes penetrate the endothelium in a paracellular manner, neighboring ECs detach. It is generally believed that the detachment of the two, or sometimes more, adjacent ECs is triggered by the loss of *trans*-VE-cadherin interactions, ^{4,5} although VE-cadherin may also be redistributed, like a "trap-door" mechanism.^{6,7}

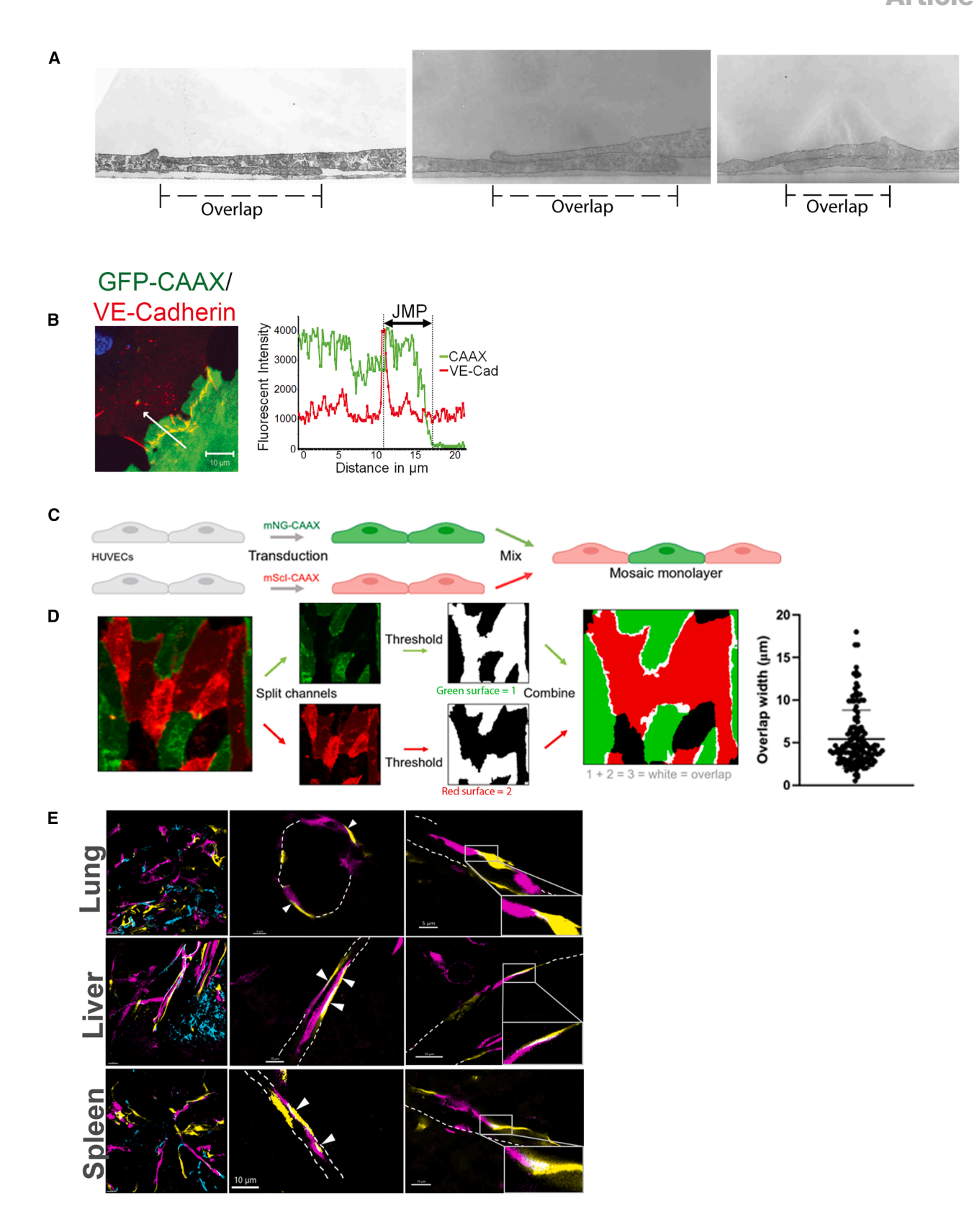
Several previous structural studies focusing on the architecture of the vessel wall using transmission or scanning electron microscopy (EM) revealed that the ECs do not simply lie side by side, like a sheet of epithelial cells, but, in fact, partially overlap.

But the membrane from one EC protrudes underneath the membrane of the neighboring EC.

But the membran







Article



beds from a Confetti-knockin mouse model, we found these overlaps to be present in the vascular beds of the lung, liver, spleen, retina, and cremaster muscle. In vitro transmission EM images confirmed the overlaps in EC cultures. Using fluorescently membrane-labeled mosaic EC monolayers, we found that in a monolayer, virtually all ECs overlap and function as preferred exit sites for leukocytes during inflammation. Realtime confocal and lattice light-sheet microscopy (LLSM) revealed that leukocytes squeezed themselves through the overlapping endothelial membranes using a so-called "TEM tunnel." Detailed analysis revealed that leukocytes lifted the membrane of the upper EC and crawled over and indented the membrane of the underlying EC, establishing a membrane tunnel through which the leukocytes squeezed. Differential dynamics of the junctional proteins VE-cadherin and PECAM-1 were found in this tunnel structure. Whereas VE-cadherin is excluded from the dissociated membranes and only present on the sides of the tunnel where the endothelial membranes are still connected, PECAM-1 was seen to decorate the entirety of the tunnel both in vitro and in vivo.

Taking these results together, we show here for the first time the true 3D architecture of paracellular TEM events. Specifically, our findings reveal that ECs do not simply dissociate from each other but rather form a membrane-based transmigration tunnel that allows leukocytes to migrate through. These findings enhance our understanding of the spatiotemporal profile of paracellular leukocyte transmigration and present novel means through which endothelial cellular structures support leukocytes in breaching the endothelial monolayer.

RESULTS

EC membranes overlap in vivo and in vitro

To examine the morphology of ECs in a monolayer, we used transmission EM and found that endothelial membranes of cultured ECs partially overlap at junction regions (Figure 1A), in so-called fork-like overlaps and single overlaps (Figure S1A). Despite the different morphological phenotypes, the overlaps showed an average width of around 4 μ m. These data are in line with other studies that revealed the existence of EC overlaps *in vivo* in rat airways. ^{11,12} Using a fluorescent protein with a plasma membrane anchor (CaaX), we confirmed that one EC protruded beyond the VE-cadherin lining (Figure 1B). We found similar overlaps in human artery ECs (Figure S1B). To charac-

terize the dynamics of the endothelial membrane overlap, two populations of ECs were transduced with either mNeonGreen-CaaX or mScarlet-CaaX, and a mosaic endothelial monolayer was generated (Figure 1C). Alternatively, we used mTurquoise2-CaaX and YFP-CaaX with similar results. For quantification, confocal z stacks were processed by thresholding the maximum projection of each color channel and quantifying the overlap between the two channels. The result is an overlap of 4–5 μm, comparable to what was measured with the electron microscope (Figure 1D). We additionally used a vessel-on-a-chip model¹⁴ to mimic human physiology more closely and found the presence of endothelial membrane overlaps (Figure S1C). To study whether endothelial membranes overlapped in different vascular beds in vivo, we used the Confetti $^{\rm fl/wt} \rm Cdh5^{\rm CreERT2}$ mice to induce endothelium-specific stochastic expression of membrane-bound CFP and cytosolic YFP/RFP.¹⁵ We detected overlapping endothelial membranes in the lung, liver, and spleen (Figure 1E) as well as the cremaster muscle (Video S1). Moreover, we found overlapping endothelial membranes in the inflamed retinas of cynomolgus monkeys (Figure S1D). 16 These data indicate that endothelial membrane overlaps can be found in different vascular beds

Overlapping membranes depend on actin regulation and are favored for TEM

To investigate the dynamics of the endothelial overlap, we followed mosaic EC monolayers in time, quantified the overlap width, and found that the overlap remained stable at around 4 μm for at least 60 min (Figure 2A). To study whether the actin cytoskeleton regulates EC overlap, we used small-molecule inhibitors. These inhibitors were administered to CaaX-expressing mosaic EC monolayers, and the overlap dynamics were recorded in real time. The results showed that blocking actin regulation reduced the overlap width, ultimately resulting in a loss of cell-cell contacts and gap formation (Figure 2B). Interestingly, blocking Rho-kinase also resulted in a reduction in the overlap region, indicating that both myosin-mediated actin contractility and regulation of actin turnover are necessary for the dynamics of endothelial membrane overlap.

Next, we investigated the distribution of junctional proteins covering the EC overlap. We found that PECAM-1 covered over 70% of the overlapping areas, whereas VE-cadherin and JAM-A covered only 15% of the overlap (Figure 2C). However, when PECAM-1 was depleted, we observed no change in overlap width

Figure 1. Adjacent EC membrane overlap

(A) Transmission electron microscopy is used to show overlapping endothelial membranes (dashed lines). Representative images are shown of three separate experiments with 15 junctions imaged in total. The average junctional width of these overlaps is approximately 4 µm.

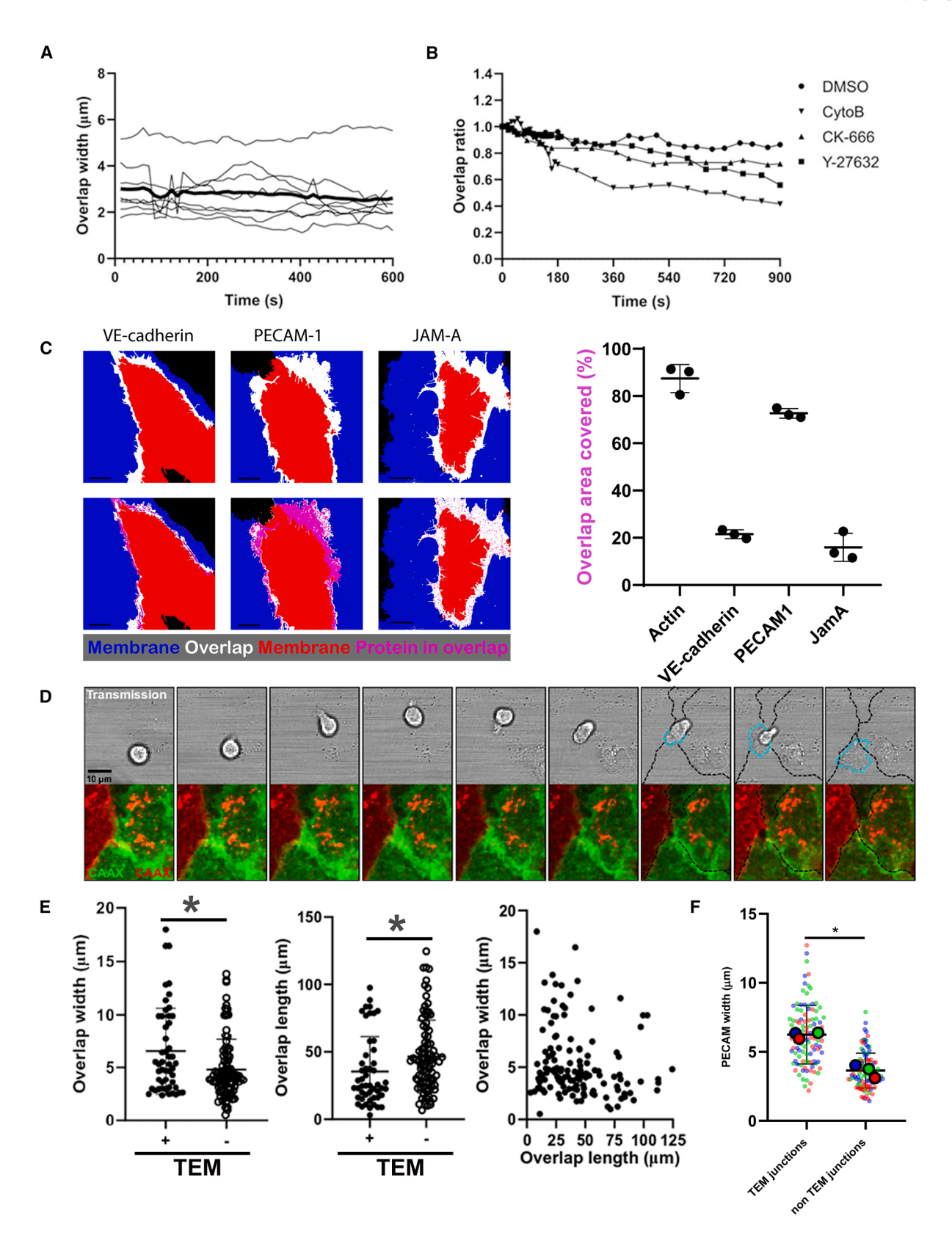
(B) HUVECs transfected with membrane marker CaaX-GFP (green) and stained for VE-cadherin (red). Image shows two neighboring ECs, one transfected with CaaX (green) and one wild-type (WT) EC (red background stain from antibody). The membrane continues beyond the VE-cadherin stain, shown by the green signal of the CaaX transfection. A representative image of three separate experiments with >10 junctions imaged per replicate. The graph on the right shows the intensity profile of the arrow, with VE-cadherin in red and the membrane in green. The overlap is marked as JMP (junctional membrane protrusion). Bar, 10 µm. (C) Schematic drawing of generation of mosaic endothelial monolayers. Mosaic monolayers were obtained by mixing two pools of HUVECs that were transduced with CaaX fluorescently labeled with either one of the color combinations mNeonGreen/mScarlet or YFP/mTurquoise2.

(D) Maximum projections of confocal z stacks were split into separate channels. The resulting binary images were assigned different values, after which the images were summed to reveal overlapping surfaces. The mean overlap width of CaaX-expressing HUVECs is 5.4 μ m. n = 142 junctions, 4 independent experiments (Mann-Whitney U test).

(E) Confetti^{fl/wt}Cdh5^{CreERT2} mice were used to study EC overlap in the lung, liver, and spleen. Displayed are red fluorescent protein (magenta), yellow fluorescent protein (yellow), and cyan fluorescent protein (cyan). Overlapping ECs are detected in the different organs as indicated by arrows.







(legend on next page)



(Figure S2A), indicating that PECAM-1 marked the overlaps but was not required for their formation. Treating EC monolayers with tumor necrosis factor alpha (TNF-α) induced an elongated EC morphology, an established inflammatory phenotype, ¹⁷ but did not influence the dynamics or width of the overlaps (Figure S2B). Visualizing neutrophil transmigration over mNeon-Green/mScarlet-CaaX-expressing mosaic endothelial monolayers using confocal microscopy imaging, both transmitted light (Figure 2D, top) and fluorescence (Figure 2D, bottom), allowed us to analyze the correlation between neutrophil diapedesis sites and endothelial overlap width. Remarkably, when focusing on TEM events, we found that neutrophils preferred to cross shorter EC junctions at areas with wider overlaps (Figure 2E). We were able to verify this using a non-blocking PECAM-1 antibody, observing that junctions with wider PECAM-1 distribution were preferred as well for neutrophil TEM (Figure 2F). This is in line with the fact that PECAM-1 covered over 70% of the membrane overlap area (Figure 2C). Moreover, junctions that supported TEM were significantly shorter in length than non-TEM junctions within the same monolayer (Figures 2E and S2C). Interestingly, endothelial membrane overlap width and length were slightly, yet significantly, inversely correlated (Figure 2E). These results indicate that the shorter sides of elongated inflamed ECs overlapped more. It has been suggested that tricellular junctions may act as TEM hotspots for neutrophils when crossing endothelial monolayers. 18,19 We found that neutrophils crawled, on average, 15 µm before crossing a junction (Figure S2D). Almost all neutrophils crossed the first junction they encountered, and some preference for tricellular junctions was detected, although the difference was not significant (Figure S2D).

Overlapping membranes form a tunnel to allow paracellular diapedesis

To accurately capture all structural changes of both cell types, i.e., the leukocyte and the EC, during the extravasation process, it is required to use extremely fast data acquisition at a high-resolution level. We used confocal resonant scanning to increase the acquisition speed in 3D significantly²⁰ and applied volume rendering software analysis on the raw data to increase the visibility and interpretation of the data (Figure S3A). We found that the overlapping endothelial membranes formed a tunnel-like

structure as the neutrophils crossed (Figure 3A, left; Video S2 and S3). All TEM events that were detected showed the presence of such TEM tunnels (Figure 3A, right). The average diameter of nine tunnels imaged over three separate experiments was $5.5 \mu m$, in line with the gap size that has been measured in 2D TEM assays by us and others *in vitro*, 5,11,21,22 as well as *in vivo*. ²³ Moreover, we observed that ECs were not dissociating from each other but rather were lifted by the neutrophil to form the TEM tunnel (Figure 3B; Video S4).

To investigate these endothelial membrane structures during TEM with the highest possible spatial and temporal resolution, data were acquired using LLSM.²⁴ In comparison to the point illumination of the confocal microscope, LLSM illuminates an entire sheet. The sheet is applied at an angle relative to the sample and can be moved to cover the entire sample (Figure S3B). This type of illumination allows fast scanning through the entire sample, providing detailed spatial information in the x, y, and zdirections, with low phototoxicity. ECs stably expressed one of the CaaX-membrane markers and were grown into a mosaiclike monolayer. Data processing involves an automated deskew and deconvolution step²⁴ (Figure S3C). The volumerendered data showed the cell surface in great spatial detail, especially the overlapping EC membranes (Figure S3D). These membrane structures were difficult to capture using regular confocal microscopy, with LLSM obtaining a Z resolution of around 300 nm, depending on the mode used,²⁴ while confocal microscopy typically has a limit of 500 nm in the z direction.²⁵

The recordings showed that as a neutrophil arrived on an EC that displayed a membrane protrusion underneath its neighboring cell, the overlapping top EC membrane protrusion was lifted, facilitating the neutrophil migration underneath the upper EC (Figure 3C). This occurred rapidly within 2 min, during which both ECs covered the migrating neutrophil (Figure 3D). The two images on the right of the figure show the TEM event without the upper EC and without the upper EC and neutrophil, respectively, showing that the lower EC partly covers the neutrophil.

For all events observed, at the basolateral level, an endothelial sheet was presented to the transmigrating neutrophil (Figure 4A; Video S5). The pore exclusively appeared when the neutrophil was present between the ECs, indicating that the neutrophil initiated the pore opening. The endothelium immediately started

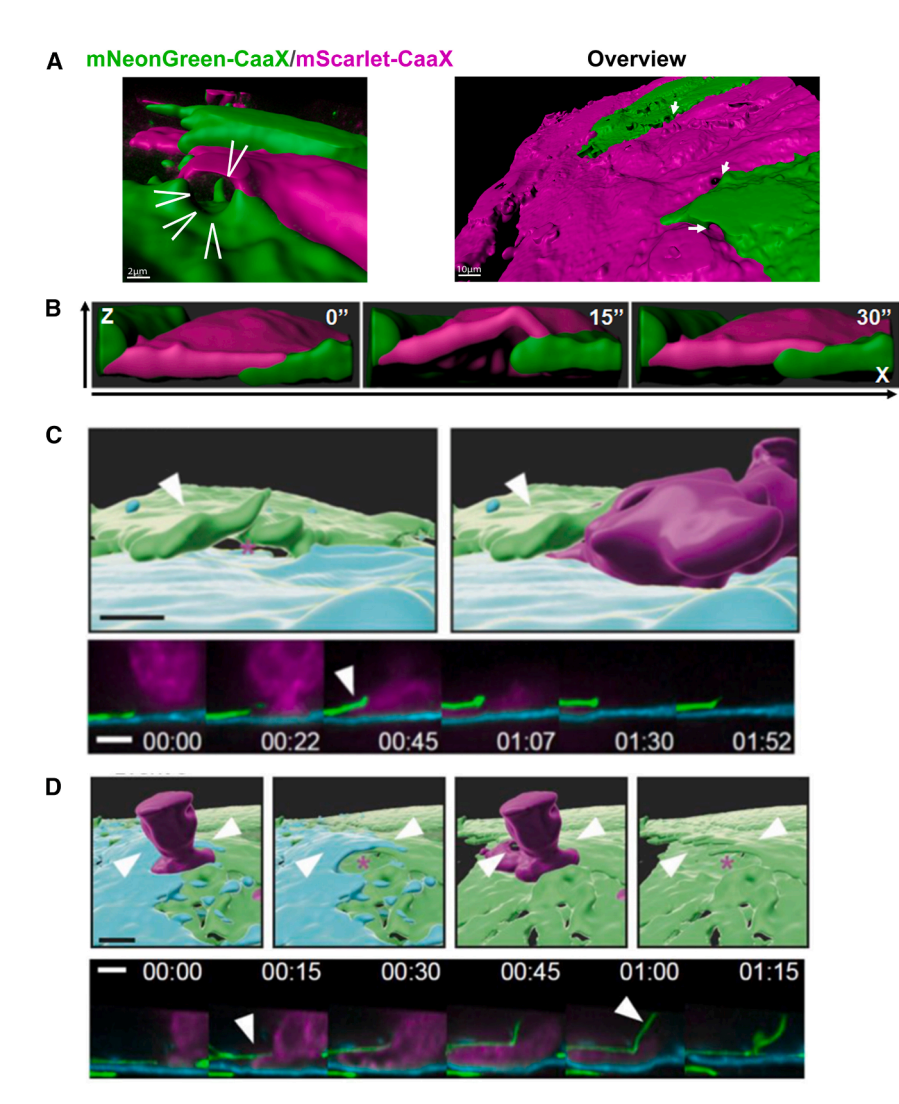
Figure 2. Characterization of the endothelial overlap

(A) Endothelial overlap width of individual junctions and their average (thick line) quantified over time. N = 9:3 junctions per time series in 3 separate experiments. (B) Overlap width of TNF- α inflamed HUVECs quantified over time upon actin (CytoB [inhibitor to actin polymerization by blocking the growing plus end of actin filaments] or CK-666 [Apr2/3 complex inhibitor, preventing actin polymerization]) or Rho-kinase (Y-27632, inhibitor of the Rho pathway, resulting in reduced actomyosin contractility) inhibition. All these inhibitors are added to the ECs only. Overlap quantified as a relative ratio to t = 0 pre-treatment, N > 5 junctions per condition.

- (C) The quantification of junctional protein coverage of the overlap area is shown in percentage. Data consist of 3 independent experiments, with 10–15 overlap areas per replicate. Dots represent the mean of each replicate (unpaired, two-tailed Student's t test). Data are represented as mean ± SEM.
- (D) Confocal microscopy images of a transmigrating neutrophil through mosaic HUVEC monolayer grown in a perfusion slide. Top: transmission images of one confocal Z slice; bottom: overlay of maximum projections of confocal z stacks of mScarlet- and mNeonGreen-Caax. Stills from time series, 40 s apart.
- (E) The overlap width of TEM event junctions (+, n = 50) is significantly wider compared to non-TEM event junctions (-, n = 92) over 6 independent experiments (Mann-Whitney, p = 0.0242). The length of these TEM event junctions is significantly shorter compared to non-TEM junctions (Mann-Whitney, p = 0.00037). Overlap length and width are negatively correlated (Pearson r = -0.18, p = 0.0324), indicating that shorter overlapping areas are wider. Data are represented as mean + SEM

(F) HUVEC monolayers stimulated with TNF- α for 4 h and, stained with non-blocking PECAM1 antibody, comparing PECAM width of TEM event junctions (N = 102) versus non-TEM event junctions (N = 108). Colors indicate the three replicates, small dots represent individual junctions, and big dots their average. PECAM width is significantly wider at TEM event junctions compared to non-TEM event junctions (unpaired t test, p = 0.001). Data are represented as mean \pm SEM.





closing the pore once the neutrophil had passed (Figure 4B; Video S5). Interestingly, it was observed that both the top and the bottom EC contributed to the formation of the TEM tunnel. The bottom EC showed protrusions that acted as pillars and were attached to the top EC that formed the ceiling of the tunnel (Figure 4C, top: Video S5 and bottom: Video S6). Although it is difficult to analyze in even greater detail, these structures may include focal adhesion sites, which we have shown are physical obstacles to neutrophils.²⁶

Previously, our lab showed that endothelial junctional membrane protrusions (JMPs) are linked to neutrophil TEM hotspots. Therefore, we concentrated in more detail on these structures before, during, and after diapedesis. Some protrusions at diapedesis sites were characterized as JMPs (Figure S4A; Video S7), while other protrusions at diapedesis sites showed a more finger-like or filopodia appearance (Figure S4B; Video S8). Additionally, we observed the combination of both structures (Figures S4C–S4E: Videos S9 and S10). In every case, diapedesis events were accompanied by active membrane structures that originated from the ECs.

Figure 3. Overlapping endothelial membranes form a tunnel structure upon extravasation of neutrophils

(A) Surface-rendered still from confocal microscopy movie showing multiple tunnel structures (white arrows) formed at the moment of neutrophil (data not shown) diapedesis through a monolayer transduced with mScarlet-CaaX and mNeon-Green-CaaX. Scale bar, 10 μm. Zoom shows the transduced cell (magenta) forming the top and the mNeonGreen-CaaX transduced cell forming the bottom of a tunnel. Scale bar, 2 μm. Representative stills of 9 events from three independent experiments. See also Videos S2–S4.

- (B) Orthogonal slice view of tunnel formation during diapedesis of neutrophil (data not shown).
- (C) Representative still (26 events captured) from a lattice light-sheet microscopy movie showing tunnel formed by underlying (turquoise) and upper (green) EC as a neutrophil (magenta) extravasates, with orthogonal slice showing the non-rendered signal. Scale bars, 5 μm .
- (D) Still from a lattice light-sheet microscopy movie showing tunnel formed by underlying (green) and upper (turquoise) ECs as neutrophil extravasaates (two left images). Images on the right show the TEM event with only the bottom EC and neutrophil and with only the bottom EC. Arrows indicate parts of EC membranes that cover the neutrophil mid-diapedesis, and the asterisk indicates neutrophil location. The bottom image shows the orthogonal slice view of the non-rendered signal. Scale bars, 5 µm.

Diapedesis events can combine the para- and transcellular routes

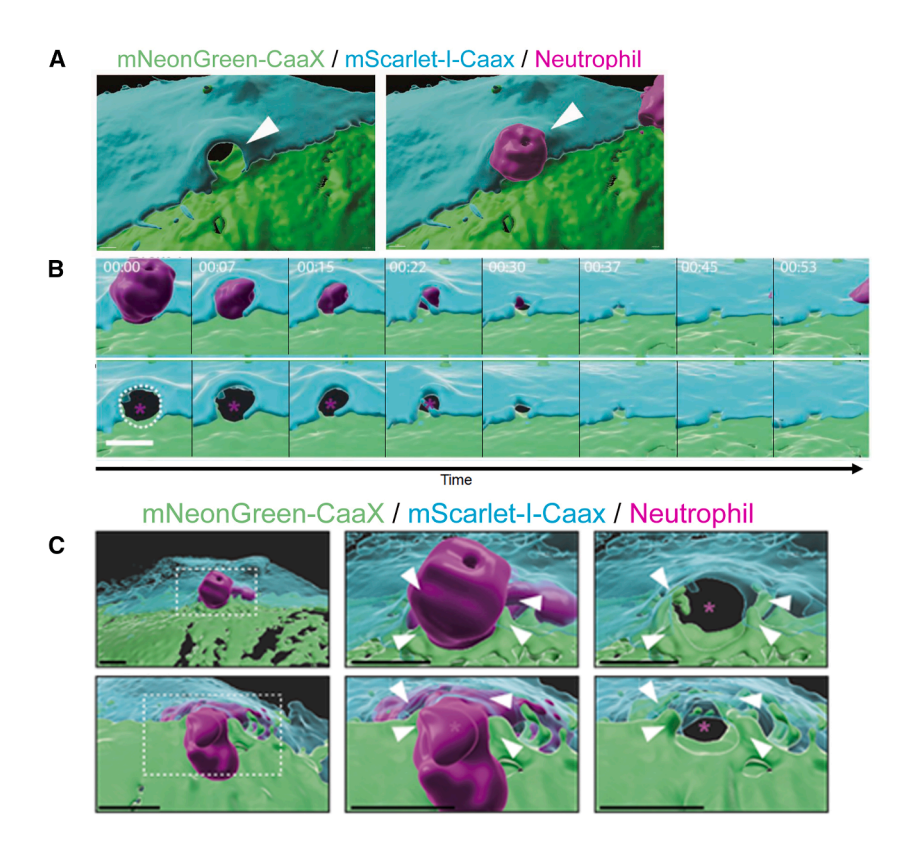
Already in the nineties, Butcher and Springer described several well-defined stages of transmigration, including rolling, adhesion, crawling, and diape-

desis.^{2,3} They discriminated between the transcellular and paracellular diapedesis routes. Interestingly, we observed several events that cannot be categorized in either of the two routes. In some cases, diapedesis appeared close to a junction but not at a junction. Yet, both ECs contributed by inducing dynamic membrane structures, whereas the tunnel pore seems to be made by only one of the two ECs (Figures 4D and 4E; Video S11).

Junctional protein dynamics in the TEM tunnel

As most neutrophils prefer the paracellular route to cross the endothelium, and as neutrophils made their way through an endothelial tunnel when transmigrating, we questioned how the proteins involved in leukocyte TEM were distributed during this event. We found that ICAM-1 was distributed along the tunnel, supporting the transmigration route of the neutrophil (Figure 5A), following previous work.²⁹ These data were recorded with a regular confocal microscope. Moreover, we found that PECAM-1 was distributed in a ring-like structure around the neutrophil when starting to penetrate (Figures 5B and S5A). This is in line with other studies.^{30–32} Using Airyscan imaging, we





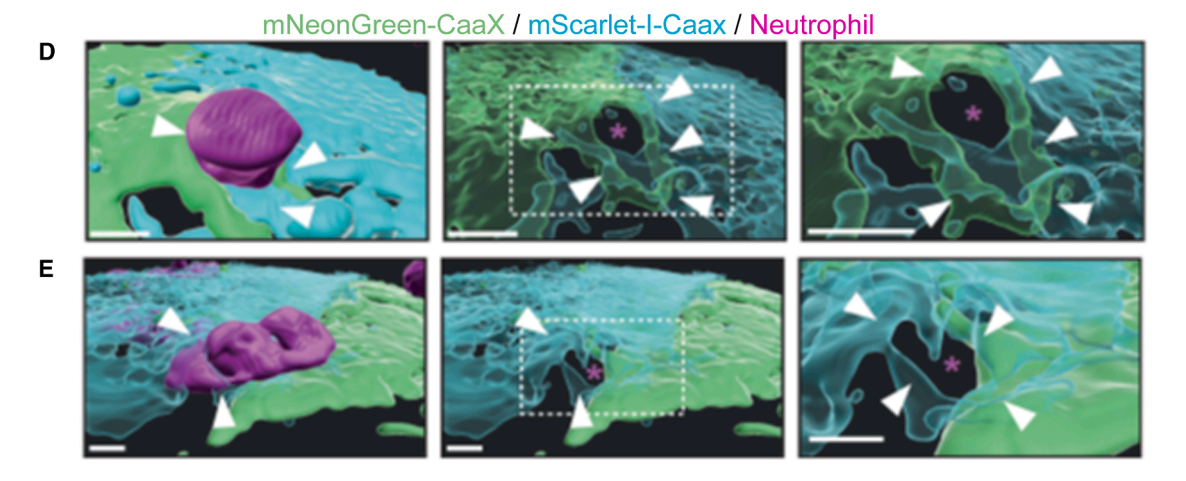


Figure 4. TEM tunnel dynamics and architecture

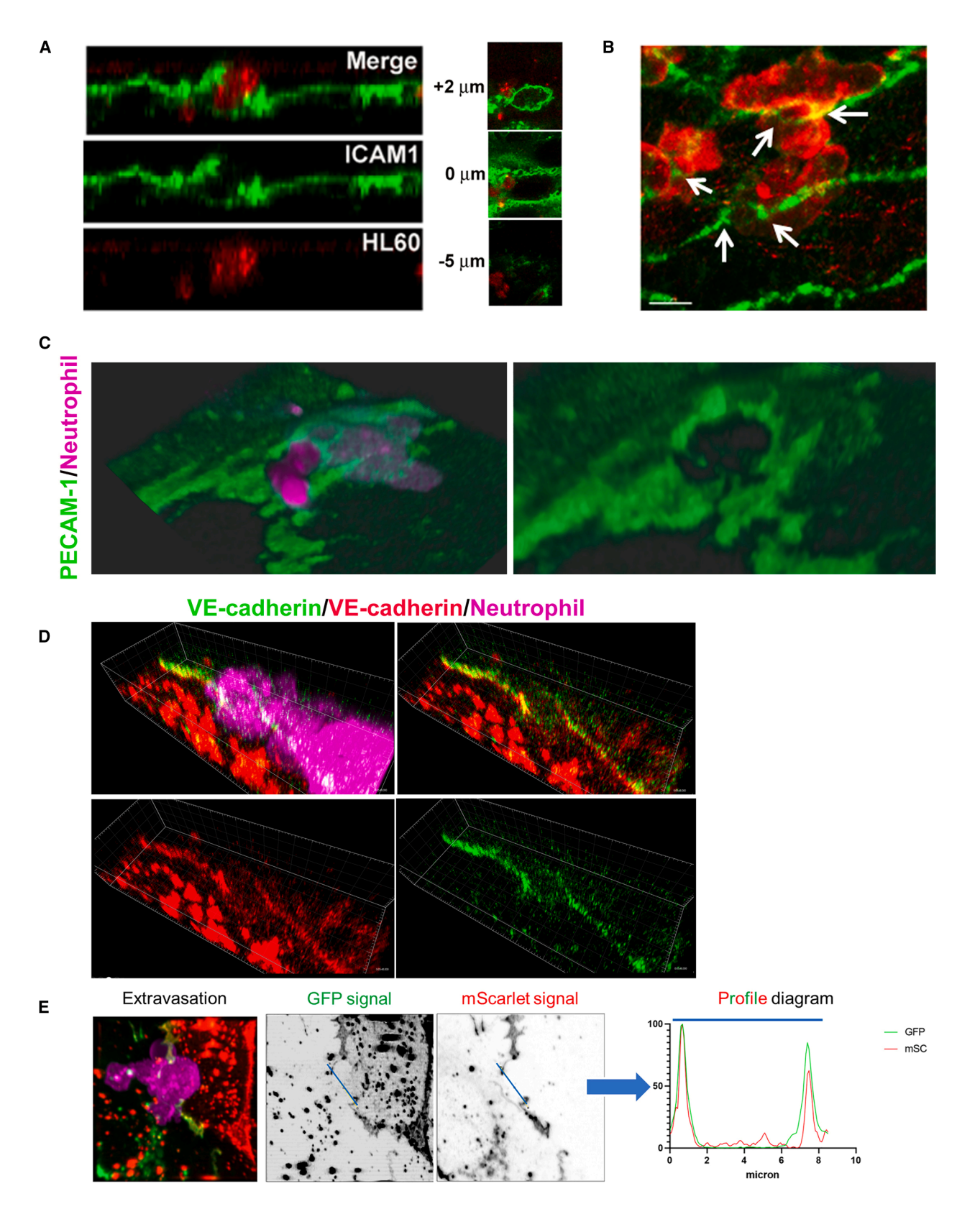
(A) Surface rendering of endothelial membranes (turquoise, green) forming a TEM tunnel at the moment a neutrophil (magenta) is in mid-diapedesis imaged using lattice light-sheet microscopy (LLSM).

(B) Surface rendering of endothelial membranes (turquoise, green) and their temporal dynamics during the closing of TEM tunnel.

(C) Surface rendering of two TEM events, showing the endothelial membranes (turquoise, green) forming a TEM tunnel as a neutrophil (magenta) moves through. Middle images are zoom-ins of the left image, with white arrows indicating the pillar structures of the bottom EC contributing to the walls of the tunnel; the right image shows only the endothelial membranes, with an asterisk indicating neutrophil location.

(D and E) Paracellular-transcellular TEM events show aberrant membrane configuration. Two examples of transmigration events that cannot be classified as either para- or transcellular diapedesis with endothelial membranes (turquoise, green) and transmigrating neutrophil (magenta). These events show tunnels with a more complicated architecture compared to the "simple" bottom and top cell configuration of TEM tunnels classified as paracellular. 26 TEM events were captured using the LLSM technique.





(legend on next page)

Article



found that PECAM-1 decorated the inside of the TEM tunnel, suggestive of support during the diapedesis step (Figure 5C; Video S12). For VE-cadherin, we noticed that it was locally dispersed and only present on the sides of the tunnel (Figure S5B), in line with previous work from us and others. ^{7,33,34} By using 2 different FP-tagged VE-cadherin constructs, each transfected in adjacent ECs, we generated a mosaic monolayer of fluorescently tagged VE-cadherin-positive EC-cell junctions and confirmed local dispersion of VE-cadherin at sites of diapedesis. Interestingly, when leukocytes penetrated the junction, we found that VE-cadherin remained co-localized adjacent to diapedesis sites. We did not detect single-colored VE-cadherin, indicating that VE-cadherin trans-interactions were maintained during diapedesis, at least at the edge of the TEM tunnels (Figures 5D and S5C). No single-colored VE-cadherin was detected at the TEM tunnel edges, indicating that VE-cadherin as a trans-interacting complex is pushed aside rather than a loss of VE-cadherin trans-interactions (Figure 5E). To show that single-colored VE-cadherin can be detected in this setup, ECs were treated with EGTA to chelate calcium, as VE-cadherin trans-interactions depend on calcium. As a result, VE-cadherin-trans interactions dissociate into single-colored ones, whereas short-term thrombin treatment did not (Figure S5D; Video S13). These data suggest that the lateral membrane mobility of VE-cadherin, rather than its ability to dissociate, is a prerequisite for efficient leukocyte paracellular TEM.

TEM tunnels decorated by PECAM-1 are observed in vivo

To study the TEM tunnels upon inflammation in vivo, we analyzed neutrophil diapedesis in inflamed murine cremaster muscles, as observed using a 4D imaging platform with advanced spatial and temporal resolution.32 Cremaster muscles were inflamed via transient induction of ischemia of the testes followed by restoration of blood flow and recording of neutrophil/vessel interactions in postcapillary venules, according to Barkaway and Rolas et al.³⁵ Breaching of venular walls was investigated in real time using neutrophil reporter mice Lyz2-EGFP-ki (display GFP^{bright} neutrophils) and following staining of EC-cell junctions by locally administered non-blocking anti-PECAM-1 antibodies. 32 Neutrophil extravasation was captured in real time (Figure 6A; Video \$14). To analyze TEM events in more detail, we used Imaris software to generate an iso-surface of PECAM-1 staining. We found that neutrophils crossed the endothelial layer through thick PECAM-1-positive regions, similar to the observations detected using in vitro models (Figure 6B). The presence of PECAM-1

around the entire extravasating neutrophil indicated the presence of endothelial membranes both above and below the migrating neutrophil (Figure 6C; Video S15). Collectively, these results support the concept that neutrophils cross the endothelial monolayer by using membrane-based tunnels through two layers of adjacent ECs.

DISCUSSION

During inflammation, circulating leukocytes cross the inflamed endothelial monolayer in a process called TEM. Neutrophils and monocytes mainly cross the endothelium in a paracellular manner, i.e., using the junctional route. It is the dogma in the field that adjacent ECs transiently physically dissociate to allow leukocytes to pass and that EC borders start and stop at VE-cadherin localization.^{4,7} However, we and others never observed that endothelial membranes retracted upon leukocyte extravasation; instead, tight gaps, supported by rings of tensile F-actin bundles, are induced between two adjacent ECs to quickly close after leukocyte passage. 21,22,32 Moreover, here we show that adjacent EC membranes overlap, extending several micrometers beyond VE-cadherin, and that these overlapping membrane areas are favored by neutrophils to cross the endothelial barrier. The finding that EC membranes overlap is not new; in fact, it has been recognized already for years.8-10 The McDonald lab documented this phenomenon in vivo using scanning EM, showing that ECs from postcapillary venules of rat trachea overlap. 11-13 However, the characteristics and role of these overlaps during TEM have not previously been explored.

The opening and closing of the endothelial gap to allow the leukocyte to cross are very rapid and take no more than a couple of minutes. Monitoring the dynamics of endothelial membranes during paracellular diapedesis requires very fast image acquisition and high Z resolution. We used resonant confocal laser scanning and LLSM to study leukocyte TEM in 3D and real time and found that overlapping endothelial membranes form structures that we have termed TEM tunnels during diapedesis.

Endothelial membrane overlaps are not controlled by inflammatory stimuli like TNF- α . It is, therefore, also not likely that other inflammatory stimuli like LTB4 are controlling overlap dynamics. Recent work from our group showed that when endothelial membrane overlaps were artificially increased, using light-induced recruitment of the RacGEF Tiam1 to the membrane to locally activate the small GTPase Rac1, a rapid increase in the electrical resistance of endothelial monolayers was measured. 36

Figure 5. Distribution of junctional proteins in TEM tunnel

(A) ICAM-1 is shown to decorate both the top and the bottom EC of a TEM tunnel induced by a transmigrating HL60 cell in red.

(B) PECAM-1 staining in green shows ring-like distribution around transmigrating neutrophil (in red). Arrows point to ring-like PECAM-1 structures. A representative image of 10 events from two separate experiments is shown.

(C) Representative still from a confocal movie of a neutrophil (magenta) transmigrating through a PECAM1-mNeonGreen (green)-expressing HUVEC monolayer. Two independent experiments. See also Video S12.

(D) Still from a movie of a neutrophil (magenta) transmigrating through an endothelial junction, with the top right cell expressing VE-cadherin-GFP (green) and the bottom left cell expressing VE-cadherin-mScarlet (red). See also Video S13.

(E) Representative (three independent experiments, 9 events) fixed transmigration event showing a neutrophil (magenta) during the diapedesis step, with the right EC expressing VE-cadherin-mScarlet (red) and the left EC expressing VE-cadherin-GFP (green). The fluorescent signal of both FPs was plotted on a line drawn across this transmigration event, showing the signals of both FPs on the sides of the TEM tunnel directly on top of each other.





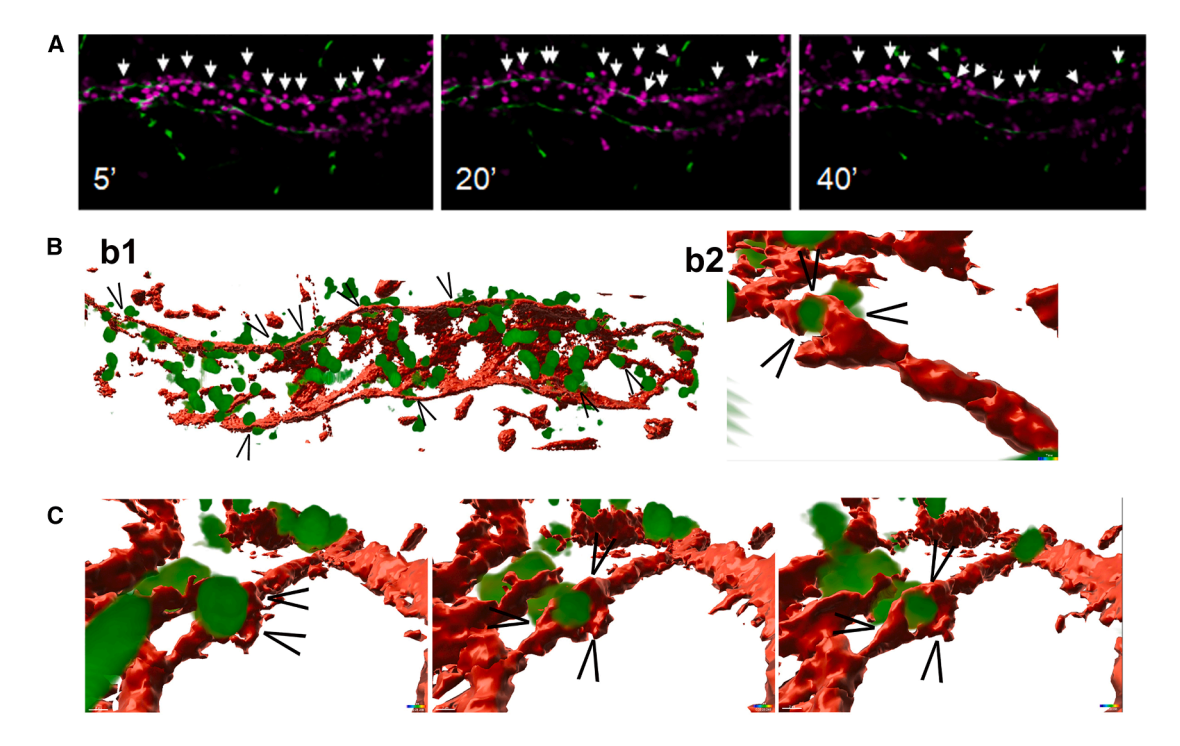


Figure 6. Spatiotemporal dynamics of PECAM-1 during leukocyte extravasation in vivo

Cremasteric venules of *LysM-EGFP-ki* mice (exhibiting GFP^{high} neutrophils) were immunostained *in vivo* for EC junctions with intrascrotal (i.s.) injection of Alexa Fluor-555-labeled anti-PECAM-1 monoclonal antibody (mAb) (PECAM-555; 4 μg/mouse; shown in red). Inflammation was induced by transient ischemia of the testes (40 min), followed by blood flow restoration and recording of neutrophil/vessel interactions in postcapillary venules.

(A) Images show a postcapillary venular segment post-reperfusion at different times (t = 5, 20, and 40 min post-reperfusion), showing the development of an inflammatory response with neutrophils in magenta and PECAM-1 in green. White arrows indicate extravasating leukocytes.

(B and C) Neutrophil (green) extravasation through endothelial junctions labeled for PECAM-1 (red) show the presence of PECAM-1 all around the transmigrating leukocyte. Images are representative of at least 6 independent experiments involving 6 mice.

Additionally, when inducing a JMP in only one of the two adjacent ECs, we found that these JMPs function as TEM hotspots for leukocytes.²⁸

A picture emerges that suggests that TEM events occur at areas of high endothelial membrane dynamics: the EC on top of the overlap shows increased protrusion activity, recognized by the crawling leukocyte, followed by a continuation of migration of the leukocyte on the bottom EC, thus generating an endothelial-based membrane tunnel that supports leukocyte crossing. Interestingly, and in line with the idea that TEM events prefer high EC membrane dynamics, increased EC membrane flaps, supporting an exaggerated and faster level of neutrophil TEM (e.g., the formation of hotspots), is a feature of autophagy-deficient ECs. Texture Strong and numerous inflammatory conditions, these findings offer a pathophysiological setting under which the presence of EC membrane flaps is pronounced.

The formation and stability of membrane overlaps do not depend on either of the junctional proteins investigated here: PECAM-1 and VE-cadherin. Whereas PECAM-1 is found to decorate the TEM tunnel, VE-cadherin is excluded from the tunnel and displaced to the sides. After the passage of the leukocyte, the two endothelial membranes connect again, and VE-cadherin redistributes to the junction. It was already suggested that a maximized contact surface between ECs and leukocytes

would limit vascular leakage during TEM.⁴ This offers another argument for the preference of transmigrating leukocytes for wide overlapping junctions. Indeed, we observed that leukocytes prefer transmigrating through wider PECAM-1-positive junctions *in vitro* and *in vivo*, underscored by our previous work and that of others.^{34,37}

Barreiro and colleagues were the first to describe endothelial membrane structures, which they termed "docking structures," primarily observed during the adhesion phase of leukocyteendothelium interactions. 38 This was followed by a study by Carman and co-workers, who identified similar structures during the diapedesis phase as leukocytes actively crossed the endothelial barrier, referring to them as "transmigratory cups." Our group subsequently investigated the molecular mechanisms governing the formation of these structures, designating them as "apical cup structures." In this work, we identified the guanine nucleotide exchange factor SGEF and its downstream effector, the small GTPase RhoG, as key regulators of their formation. 40 Further in vivo studies by the Kubes laboratory described these structures as "dome structures" and demonstrated the role of LSP1 in their regulation. 41,42 The reduction of LSP1 expression in ECs resulted in increased permeability during TEM, suggesting that the structures regulated local permeability during TEM. While subsequent studies by various research groups have further characterized these endothelial membrane formations,

Article



the use of diverse nomenclature has complicated efforts to define their precise role in leukocyte transmigration.

A major challenge in studying these structures is their highly transient nature. They form dynamically and exist only momentarily as leukocytes undergo TEM. The TEM process itself is rapid, typically occurring within 2 min for neutrophils. Capturing these fleeting events in real time has historically been difficult due to limitations in imaging technology. Until recently, most studies relied on fixed samples or 2D imaging, which, while informative, provided only a partial view of the dynamic process of leukocyte extravasation.

In this study, we employed LLSM to visualize leukocyte TEM in four dimensions with unprecedented resolution, rapid acquisition rates, and minimal phototoxicity. This imaging approach yielded novel insights, revealing the existence of an actual tunnel through which leukocytes migrate. Moreover, by using heterogeneous endothelial labeling, we were able to distinguish overlapping membranes of adjacent ECs, a level of spatial resolution not previously achieved. This methodological advancement allowed for a more precise visualization of leukocyte movement through the endothelial barrier and provided further clarity on the transient membrane structures described in previous studies. Based on our findings, we propose that the structures observed in our study are functionally and morphologically comparable to those previously reported and are likely to function in controlling permeability during leukocyte TEM.

Although LLSM is currently the state of the art for measuring fast biological processes in real time in Z, image processing, which includes de-skewing, deconvolution, and volume rendering, is still required due to the angled light-sheet illumination. Additionally, during TEM, neutrophils disturbed the light sheet and created shadow-like patterns on the endothelium that could not be corrected. Neutrophils are highly granularized, as they contain many inflammatory mediators in vesicles that can be secreted when pathogens are encountered. Unfortunately, these structures caused small deflections in the light sheet. We were not in the position to use other leukocyte types that are known to have fewer granules, e.g., T-lymphocytes or monocytes, but such experiments may be carried out in the future.

Altogether, the results of this study define the multicellular architecture of paracellular TEM, providing a 3D context in which findings on this process can be placed.

Limitations of the study

This study shows that ECs form membrane tunnels, facilitating paracellular neutrophil transmigration, but several limitations should be considered. The observations are primarily limited to neutrophils and may not extend to other leukocyte subsets, and the *in vitro* and *in vivo* models used may not fully recapitulate the complexity of *in vivo* vascular environments, including the influence of flow, perivascular structures, and organ-specific endothelial characteristics. While the study identifies actin polymerization as a regulator of membrane overlaps, the precise molecular mechanisms and signaling pathways involved remain incompletely understood and require further study. No difference in sex, gender, or both on the results of the study can be made as cells from pooled donors have been used.

RESOURCE AVAILABILITY

Lead contact

Further information and requests for resources and reagents should be directed to and will be fulfilled by the lead contact, Jaap D. van Buul (j.d. vanbuul@amsterdamumc.nl).

Materials availability

This study did not generate new unique reagents.

Data and code availability

- Microscopy data reported in this paper will be shared by the lead contact upon request.
- This paper does not report original code.
- Any additional information required to re-analyze the data reported in this paper is available from the lead contact upon request.

ACKNOWLEDGMENTS

All videos can be found at the Zenodo platform using DOI: 10.5281/zenodo.15394401. LLSM was performed at the Advanced Imaging Center at the Janelia Research Campus of Howard Hughes Medical Institute, USA. We wish to thank Dr. Paul Kubes and Dr. Björn Petri for their valuable discussions. This work was supported by LSBR grants #1649 (A.C.I.v.S.) and #1820 (L.K.) and NWO ZonMW Vici grant #91819632 (J.D.v.B. and W.J.v.d.M.). S.N. is funded by the Wellcome Trust (098291/Z/12/Z and 221699/Z/20/Z), and L.R. is supported by funding from the British Heart Foundation (FS/IBSRF/22/25121).

AUTHOR CONTRIBUTIONS

W.J.v.d.M., A.C.I.v.S., I.K., R.O.S., Y.M., R.A.B., S.K., E.W., J.H., E.M., J.J.G. A., L.K., M.L.B.G., L.R., H.W., R.M.S., A.D., J.v.R., and M.H. performed the experiments and collected and analyzed the data. T.-L.C., M.A.N., S.N., J.G., and J.D.v.B. designed the study. W.J.v.d.M., A.C.I.v.S., and J.D.v.B. wrote the manuscript.

DECLARATION OF INTERESTS

The authors declare no competing interests.

STAR*METHODS

Detailed methods are provided in the online version of this paper and include the following:

- KEY RESOURCES TABLE
- EXPERIMENTAL MODEL AND STUDY PARTICIPANT DETAILS
 - Mouse lines
 - o Animal tissue preparation and staining
 - o Cell culture and transduction
 - Sample fixation
 - o Cytoskeleton manipulation during live imaging
- METHOD DETAILS
 - Lattice light sheet microscopy imaging
 - Neutrophil isolation
 - o Neutrophil transendothelial migration under flow
 - o Antibodies
 - o In vitro imaging
 - Confocal overlap analysis
 - Quantification of travel distance
 - o In vivo imaging of TEM tunnels
- QUANTIFICATION AND STATISTICAL ANALYSIS





SUPPLEMENTAL INFORMATION

Supplemental information can be found online at https://doi.org/10.1016/j.ceirep.2025.116242.

Received: January 16, 2025 Revised: May 14, 2025 Accepted: August 12, 2025

REFERENCES

- Wittchen, E.S. (2009). Endothelial signaling in paracellular and transcellular leukocyte transmigration. Front. Biosci. 14, 2522–2545.
- Butcher, E.C. (1991). Leukocyte-endothelial cell recognition: three (or more) steps to specificity and diversity. Cell 67, 1033–1036.
- Springer, T.A. (1994). Traffic signals for lymphocyte recirculation and leukocyte emigration: the multistep paradigm. Cell 76, 301–314.
- Vestweber, D. (2015). How leukocytes cross the vascular endothelium. Nat. Rev. Immunol. 15, 692–704.
- Wessel, F., Winderlich, M., Holm, M., Frye, M., Rivera-Galdos, R., Vockel, M., Linnepe, R., Ipe, U., Stadtmann, A., Zarbock, A., et al. (2014). Leukocyte extravasation and vascular permeability are each controlled in vivo by different tyrosine residues of VE-cadherin. Nat. Immunol. 15, 223–230.
- Alcaide, P., Newton, G., Auerbach, S., Sehrawat, S., Mayadas, T.N., Golan, D.E., Yacono, P., Vincent, P., Kowalczyk, A., and Luscinskas, F.W. (2008). p120-Catenin regulates leukocyte transmigration through an effect on VE-cadherin phosphorylation. Blood 112, 2770–2779.
- Shaw, S.K., Bamba, P.S., Perkins, B.N., and Luscinskas, F.W. (2001). Real-Time Imaging of Vascular Endothelial-Cadherin During Leukocyte Transmigration Across Endothelium. J. Immunol. 167, 2323–2330.
- 8. MUIR, A.R., and PETERS, A. (1962). Quintuple-layered membrane junctions at terminal bars between endothelial cells. J. Cell Biol. 12, 443–448.
- Reese, T.S., and Karnovsky, M.J. (1967). Fine structural localization of a blood-brain barrier to exogenous peroxidase. J. Cell Biol. 34, 207–217.
- Schneeberger-Keeley, E.E., and Karnovsky, M.J. (1968). The ultrastructural basis of alveolar-capillary membrane permeability to peroxidase used as a tracer. J. Cell Biol. 37, 781–793.
- McDonald, D.M. (1994). Endothelial gaps and permeability of venules in rat tracheas exposed to inflammatory stimuli. Am. J. Physiol. 266, L61–L83.
- Baluk, P., Bolton, P., Hirata, A., Thurston, G., and McDonald, D.M. (1998).
 Endothelial gaps and adherent leukocytes in allergen-induced early- and late-phase plasma leakage in rat airways. Am. J. Pathol. 152, 1463–1476.
- Claesson-Welsh, L., Dejana, E., and McDonald, D.M. (2021). Permeability
 of the endothelial barrier: identifying and reconciling controversies. Trends
 Mol. Med. 27, 314–331.
- Van Steen, A.C.I., Kempers, L., Schoppmeyer, R., Blokker, M., Beebe, D. J., Nolte, M.A., and van Buul, J.D. (2021). Transendothelial migration induces differential migration dynamics of leukocytes in tissue matrix. J. Cell Sci. 134, jcs258690. https://doi.org/10.1242/jcs.258690.
- Manavski, Y., Lucas, T., Glaser, S.F., Dorsheimer, L., Günther, S., Braun, T., Rieger, M.A., Zeiher, A.M., Boon, R.A., and Dimmeler, S. (2018). Clonal Expansion of Endothelial Cells Contributes to Ischemia-Induced Neovascularization. Circ. Res. 122, 670–677.
- Schlingemann, R.O., Hofman, P., Klooster, J., Blaauwgeers, H.G., Van der Gaag, R., and Vrensen, G.F. (1998). Ciliary muscle capillaries have bloodtissue barrier characteristics. Exp. Eye Res. 66, 747–754.
- Marcos-Ramiro, B., García-Weber, D., and Millán, J. (2014). TNF-induced endothelial barrier disruption: beyond actin and Rho. Thromb. Haemost. 112, 1088–1102.
- Burns, A.R., Bowden, R.A., MacDonell, S.D., Walker, D.C., Odebunmi, T. O., Donnachie, E.M., Simon, S.I., Entman, M.L., and Smith, C.W. (2000).

- Analysis of tight junctions during neutrophil transendothelial migration. J. Cell Sci. 113. 45–57.
- Dias, M.C., Odriozola Quesada, A., Soldati, S., Bösch, F., Gruber, I., Hildbrand, T., Sönmez, D., Khire, T., Witz, G., McGrath, J.L., et al. (2021). Brain endothelial tricellular junctions as novel sites for T cell diapedesis across the blood-brain barrier. J. Cell Sci. 134, jcs253880.
- Elliott, A.D. (2020). Confocal Microscopy: Principles and Modern Practices. Curr. Protoc. Cytom. 92, e68.
- Heemskerk, N., Schimmel, L., Oort, C., van Rijssel, J., Yin, T., Ma, B., van Unen, J., Pitter, B., Huveneers, S., Goedhart, J., et al. (2016). F-actin-rich contractile endothelial pores prevent vascular leakage during leukocyte diapedesis through local RhoA signalling. Nat. Commun. 7, 10493.
- Barzilai, S., Yadav, S.K., Morrell, S., Roncato, F., Klein, E., Stoler-Barak, L., Golani, O., Feigelson, S.W., Zemel, A., Nourshargh, S., and Alon, R. (2017). Leukocytes Breach Endothelial Barriers by Insertion of Nuclear Lobes and Disassembly of Endothelial Actin Filaments. Cell Rep. 18, 685–699
- Mamdouh, Z., Mikhailov, A., and Muller, W.A. (2009). Transcellular migration of leukocytes is mediated by the endothelial lateral border recycling compartment. J. Exp. Med. 206, 2795–2808.
- 24. Chen, B.C., Legant, W.R., Wang, K., Shao, L., Milkie, D.E., Davidson, M. W., Janetopoulos, C., Wu, X.S., Hammer, J.A., 3rd, Liu, Z., et al. (2014). Lattice light-sheet microscopy: imaging molecules to embryos at high spatiotemporal resolution. Science 346, 1257998.
- Schermelleh, L., Heintzmann, R., and Leonhardt, H. (2010). A guide to super-resolution fluorescence microscopy. J. Cell Biol. 190, 165–175.
- Arts, J.J.G., Mahlandt, E.K., Schimmel, L., Grönloh, M.L.B., van der Niet, S., Klein, B.J.A.M., Fernandez-Borja, M., van Geemen, D., Huveneers, S., van Rijssel, J., et al. (2021). Endothelial Focal Adhesions Are Functional Obstacles for Leukocytes During Basolateral Crawling. Front. Immunol. 12, 667213.
- Grönloh, M.L.B., Arts, J.J.G., Mahlandt, E.K., Nolte, M.A., Goedhart, J., and van Buul, J.D. (2023). Primary adhered neutrophils increase JNK1-MARCKSL1-mediated filopodia to promote secondary neutrophil transmigration. iScience 26, 107406.
- Arts, J.J., Mahlandt, E.K., Grönloh, M.L., Schimmel, L., Noordstra, I., Gordon, E., van Steen, A.C., Tol, S., Walzog, B., van Rijssel, J., et al. (2021). Endothelial junctional membrane protrusions serve as hotspots for neutrophil transmigration. eLife 10, e66074.
- Millán, J., Hewlett, L., Glyn, M., Toomre, D., Clark, P., and Ridley, A.J. (2006). Lymphocyte transcellular migration occurs through recruitment of endothelial ICAM-1 to caveola- and F-actin-rich domains. Nat. Cell Biol. 8, 113–123.
- Su, W.H., Chen, H.I., and Jen, C.J. (2002). Differential movements of VEcadherin and PECAM-1 during transmigration of polymorphonuclear leukocytes through human umbilical vein endothelium. Blood 100, 3597–3603.
- Mamdouh, Z., Chen, X., Pierini, L.M., Maxfield, F.R., and Muller, W.A. (2003). Targeted recycling of PECAM from endothelial surface-connected compartments during diapedesis. Nature 421, 748–753.
- Woodfin, A., Voisin, M.B., Beyrau, M., Colom, B., Caille, D., Diapouli, F.M., Nash, G.B., Chavakis, T., Albelda, S.M., Rainger, G.E., et al. (2011). The junctional adhesion molecule JAM-C regulates polarized transendothelial migration of neutrophils in vivo. Nat. Immunol. 12, 761–769.
- 33. van Buul, J.D., Voermans, C., van den Berg, V., Anthony, E.C., Mul, F.P.J., van Wetering, S., van der Schoot, C.E., and Hordijk, P.L. (2002). Migration of human hematopoietic progenitor cells across bone marrow endothelium is regulated by vascular endothelial cadherin. J. Immunol. 168, 588–596.
- Kroon, J., Daniel, A.E., Hoogenboezem, M., and van Buul, J.D. (2014).
 Real-time imaging of endothelial cell-cell junctions during neutrophil transmigration under physiological flow. J. Vis. Exp. e51766. https://doi.org/10.3791/51766.

Article



- Faust, N., Varas, F., Kelly, L.M., Heck, S., and Graf, T. (2000). Insertion of enhanced green fluorescent protein into the lysozyme gene creates mice with green fluorescent granulocytes and macrophages. Blood 96, 719–726.
- Mahlandt, E.K., Palacios Martínez, S., Arts, J.J.G., Tol, S., van Buul, J.D., and Goedhart, J. (2023). Opto-RhoGEFs, an optimized optogenetic toolbox to reversibly control Rho GTPase activity on a global to subcellular scale, enabling precise control over vascular endothelial barrier strength. eLife 12, RP84364.
- 37. Barkaway, A., Rolas, L., Joulia, R., Bodkin, J., Lenn, T., Owen-Woods, C., Reglero-Real, N., Stein, M., Vázquez-Martínez, L., Girbl, T., et al. (2021). Age-related changes in the local milieu of inflamed tissues cause aberrant neutrophil trafficking and subsequent remote organ damage. Immunity 54, 1494–1510.e7.
- Barreiro, O., Yanez-Mo, M., Serrador, J.M., Montoya, M.C., Vicente-Manzanares, M., Tejedor, R., Furthmayr, H., and Sanchez-Madrid, F. (2002).
 Dynamic interaction of VCAM-1 and ICAM-1 with moesin and ezrin in a novel endothelial docking structure for adherent leukocytes. J. Cell Biol. 157, 1233–1245. https://doi.org/10.1083/jcb.200112126.

- Carman, C.V., and Springer, T.A. (2004). A transmigratory cup in leukocyte diapedesis both through individual vascular endothelial cells and between them. J. Cell Biol. 167, 377–388. https://doi.org/10.1083/jcb.200404129.
- van Buul, J.D., Allingham, M.J., Samson, T., Meller, J., Boulter, E., García-Mata, R., and Burridge, K. (2007). RhoG regulates endothelial apical cup assembly downstream from ICAM1 engagement and is involved in leukocyte trans-endothelial migration. J. Cell Biol. 178, 1279–1293. https://doi.org/10.1083/jcb.200612053.
- Phillipson, M., Kaur, J., Colarusso, P., Ballantyne, C.M., and Kubes, P. (2008). Endothelial domes encapsulate adherent neutrophils and minimize increases in vascular permeability in paracellular and transcellular emigration. PLoS One 3, e1649. https://doi.org/10.1371/journal.pone.0001649.
- Petri, B., Kaur, J., Long, E.M., Li, H., Parsons, S.A., Butz, S., Phillipson, M., Vestweber, D., Patel, K.D., Robbins, S.M., and Kubes, P. (2011). Endothelial LSP1 is involved in endothelial dome formation, minimizing vascular permeability changes during neutrophil transmigration in vivo. Blood 117, 942–952. https://doi.org/10.1182/blood-2010-02-270561.





STAR*METHODS

KEY RESOURCES TABLE

REAGENT or RESOURCE	SOURCE	IDENTIFIER
Antibodies		
VE-Cadherin Mouse monoclonal IgG1 directly labeled with Af647	BD Biosciences	#561567
PECAM-1 mouse monoclonal IgG1 directly labeled with Alexa Fluor 647	BD Biosciences	#561654
JAM-A rabbit polyclonal IgG	Zymed	#36-1700
Phalloidin dye 405-l	Fisher Scientific	#16109370
Hoechst 33342	Life Technologies	#H-1399
Chicken anti-rabbit IgG Alexa Fluor 647	Invitrogen	#A12443
PECAM-1 rabbit polyclonal IgG	Santa Cruz	#sc-8306
Swine anti-Rabbit-HRP	DAKO	#P0399
Chemicals, peptides, and recombinant proteins		
Cytochalasin B	Sigma-Aldrich	#C26762
Y-27632	Calbiochem	#688000
CK-666	Sigma-Aldrich	#SML006
DMSO	Sigma-Aldrich	472301
PBS	Fresenius Kabi	#M090001/02
TNF-α	Peprotech	#300-01A
Vybrant [™] DiD Cell-Labeling Solution	ThermoFisher	V22887
Critical commercial assays		
6-channel μ-slides VI 0.4	Ibidi	#80666
Deposited data		
Zenodo platform	DOI	10.5281/zenodo.15394401
Experimental models: Cell lines		
Pooled human umbilical vein endothelial cells	Lonza	#C2519A: P1052
Experimental models: Organisms/strains		
Lyz2-EGFP-ki mice	Ludwig Maximilians University of Munich, Germany	N/A
Rosa26-Confetti x Cdh5-CreERT2 mice	-	N/A
Software and algorithms		
FIJI/ImageJ	-	(v.1,52p)
maris	-	9.7.2
Prism Graphpad	_	8.0.1

EXPERIMENTAL MODEL AND STUDY PARTICIPANT DETAILS

Mouse lines

Mice carrying the Rosa26-Confetti transgene were bred with Cdh5-CreERT2 mice to induce endothelial-specific, tamoxifen-inducible conditional Cre-recombinase expression in endothelial cells resulting in the exclusive labeling of endothelial cells with the heterogeneous labeling of the confetti construct. These confettifl/wt -Cdh5-CreERT2 mice were injected for five consecutive days with Tamoxifen (2mg/mouse) to induce sufficient recombination of the rosetta construct for imaging purposes. To preserve fluorophore function and avoid the collapse of blood vessels mice were perfused with PLP-fixation buffer before sacrifice by cervical dislocation. Mice were put into deep anesthesia using hexafluorane and the thorax was opened after which a cut to the left ventricle was made. 10 ML PLP fixation buffer was slowly injected into the left ventricle replacing the blood. After this procedure, the mouse was sacrificed by cervical dislocation, and organs were harvested. All animal experiments with the Confetti mice were conducted according to the principles of laboratory animal care and according to the German national laws. The studies have been approved by the local ethical committee (Regierungspräsidium Darmstadt, Hessen FU/1097 and FU/1000).



Animal tissue preparation and staining

Liver, lung, and spleen were further fixated overnight using 4% PFA in PBS, washed with P-buffer, and stored in 30% sucrose overnight. The organs were then put into cryo molds filled with Tissue-TEK, frozen, and stored at -80. Afterward, coupes were sliced and mounted for imaging using Prolong antifade Glass. Imaging was performed on a Leica SP8 and image analysis was performed using Imaris. All animals for the cremaster muscle experiments were group housed in individually ventilated cages under specific pathogen-free (SPF) conditions and a 12 h light-dark cycle. Animals were humanely sacrificed via cervical dislocation at the end of experiments in accordance with UK Home Office regulations. The macaque retinas were obtained as described. In brief, animal eyes were kindly provided by TNO Rijswijk and local laboratories. Institutional guidelines regarding animal experimentation were followed. The anterior segment including the ciliary body and iris were dissected from these eyes and processed for transmission electron microscopy analysis.

Cell culture and transduction

Pooled human umbilical vein endothelial cells (HUVECs; Lonza, P1052, #C2519A) were cultured at 37° C with 5% CO2 in enriched Endothelial Growth Medium (EGM2; #C-22211, Promocell) supplemented with 2% endothelial growth factor mix (#C-39216, Promocell), 100 U/mL penicillin, and 100 µg/mL streptomycin (#15140122, Gibco). Cells were cultured on fibronectin (FN; CLB) coated surfaces for up to passage 8 and tested for mycoplasm (negative). For fluorescence microscopy, cells were transduced (1:500) with lentiviral constructs to express CAAX tagged with fluorescent protein mScarlet, YFP, mNeonGreen, or mTurquoise2, and selected with 100 µg/mL puromycin in EGM2. Cells were allowed to form a confluent mosaic monolayer after mixing transduced cells 1:1 in the combinations mScarlet/mNeongreen- and YFP/mTurqoise2-CAAX to enable overlap quantification as described later. To mimic inflammation, confluent cells received 10 ng/mL human TNF- α (Peprotech, #300-01A) in EGM2 4 h prior to imaging.

Sample fixation

For antibody stainings, mosaic monolayers of two-color-CAAX-transduced HUVECs were cultured at FN-coated 12mm diameter glass imaging coverslips. Cells were fixed with 4% final concentration paraformaldehyde in phosphate buffered saline ++ (PBS, Fresenius Kabi, #M090001/02) with 1 μg/mL CaCl₂ and 0.5 μg/mL MgCl2 for 5 min at 37°C and treated with antibodies and/or dyes (as specified). Coverslips were secured on imaging slides using Mowiol mounting medium (Sigma-Aldrich).

Cytoskeleton manipulation during live imaging

Confluent mosaic monolayers of two-color-CAAX-transduced HUVECs were cultured at FN-coated 8-well μ -slides (#80826, Ibidi). F-actin modulating compounds were added in warm EGM2 to live cells during imaging at 37°C with 5% CO2 to a final concentration of 1 μ M Cytochalasin B (Sigma-Aldrich, #C26762), 10 μ M Y-27632 (Calbiochem, #688000), 100 μ M CK-666 (Sigma-Aldrich, #SML006), or 10mM DMSO (Sigma-Aldrich). Afterward, cells were fixed with PFA as described above and endothelial cell overlap was quantified using ImageJ/FIJI as described below.

METHOD DETAILS

Lattice light sheet microscopy imaging

The lattice light sheet microscope located at the Advanced Imaging Center (AIC) at the Janelia Research Campus of the Howard Hughes Medical Institute (HHMI)²⁴ was used and described previously.²⁸ In brief, HUVECs stably expressing mNeonGreen-CAAX or mScarlet-I-CAAX were cultured on FN-coated 5mm round glass coverslips (Warner Instruments, Catalog # CS-5R) for 2 days. ECs were stimulated with 10 ng/mL TNF-alpha 20h before imaging. Imaging was performed in HEPES buffer²¹ at 37 Celsius with 5% CO2 for maximally 30 min. Neutrophils were isolated as described before/below, stained for 20 min at 37 Celsius with Cell Tracker Deep Red (Invitrogen), washed and centrifuged for 3 min, 400G at room temperature, and added right above the coverslip between the excitation and detection objectives. 488 nm, 560 nm, and 642 nm diode lasers (MPB Communications) at 30% acousto-optic tunable filter (AOTF) transmittance and 50 mW initial box power and an excitation objective (Special Optics, 0.65 NA, 3.74 mm WD) were used for illumination. Fluorescence was detected via the detection objective (Nikon, CFI Apo LWD 25XW, 1.1 NA) and a sCMOS camera (Hamamatsu Orca Flash 4.0 v2). Exposure time was 20 ms with 50% AOTF transmittance and Z-step size was 0.211µm. The time interval was about 7.5 s for three-channel, 5 s for two-channel time-lapse, and 2.5 s for one-channel time-lapse. Point-spread functions were measured using 200 nm tetraspeck beads (Invitrogen cat# T7280) for each wavelength. Data was deskewed and deconvolved as described in Supplemental Methods and analyzed using Imaris software.

Neutrophil isolation

Polymorphonuclear neutrophils (PMNs) were isolated from whole peripheral blood from healthy donors. Blood was diluted (1:1) in RT PBS with 1:10 TNC, transferred onto 1.076g/mL Percoll separation medium at RT, and separated by centrifuging at RT for 20 min at 800G with start and brake at setting 3. The supernatant was removed to leave only Percoll containing the PMNs and the erythrocyte layer below. Erythrocytes were lysed in ice-cold buffer (water for injection with 155mM NH4CI, 10mM KHCO3, 0.1mM EDTA (all Sigma-Aldrich)) on ice for 5–15 min until the suspension either cleared or became dark red. Neutrophils were pelleted at 4°C for 5 min at 450G with start and brake at setting 9. Supernatant was removed and remaining erythrocytes were lysed again with





ice-cold buffer for 5 min on ice. Neutrophils were pelleted and supernatant discarded, after which neutrophils were washed with 4°C PBS and pelleted again. Neutrophils were then resuspended in HEPES+ buffer (20mM HEPES, 132mM NaCl, 6mM KCl, 1mM MgSO4, 1.2mM K2HPO4, pH7.4, 1mM CaCl2, 5mM D-glucose (all Sigma-Aldrich) and 0.4% human serum albumin (Sanquin Reagents). Primary human neutrophils were collected from peripheral blood extracted from healthy voluntary donors, employed at Sanquin in The Netherlands, that signed informed consent according to the rules maintained by the Sanquin Medical Ethical Committee, which are based on rules and legislation in place within The Netherlands.

Neutrophil transendothelial migration under flow

Confluent mosaic monolayers of two-color-CAAX-transduced HUVECs were cultured at FN-coated 6-channel μ -slides VI 0.4 (#80666, Ibidi). To mimic inflammation, cells received 10ng/mL human TNF α in EGM2 4 h prior to flow experiments. During microscopy at 37°C and 5% CO₂, channels were connected to a pump system providing a laminar flow of 0.5dyne/cm2 in 37°C HEPES+ medium. Every channel received 1 million freshly isolated neutrophils resuspended in HEPES+ medium that were activated by incubation at 37°C for 15–30 min. Neutrophils were visualized using 1:6000 DiD dye that incubated with the neutrophils during activation. Transmigration was captured for 10 min after neutrophil injection to the flow system by acquiring repeated Z-stacks with step size never exceeding 1 μ m. Fluorescence was detected with the Zeiss LSM980 AiryScan2 machine (ZEISS) with ZEN software, using the 25× water-immersion NA.8 objective at 2.5× zoom and 8× multiplex imaging settings. Endothelial cell junction overlap was quantified using ImageJ/FIJI as described, classifying junctions based on presence or absence of a neutrophil transmigration event.

Antibodies

Antibodies were used on fixed cells (see above) that were permeabilized, if necessary, 0.1% Triton X- for 5–10 min. Cells were blocked using PBS with 2% bovine serum albumin (SERVA, #11920) and incubated with primary and secondary antibody, washing coverslips with PBS++ in between permeabilization, blocking and staining steps. Antibodies and dyes used: VE-cadherin mouse monoclonal IgG1 antibody directly labeled with Alexa Fluor 647 (BD Biosciences, #561567), PECAM-1 non-blocking mouse monoclonal IgG1 antibody directly labeled with Alexa Fluor 647 (BD Biosciences, #561654), JAM-A rabbit polyclonal IgG antibody (Zymed, #36–1700), Phalloidin labeled with Fluorescence dye 405-I (Fisher Scientific, #16109370), Hoechst 33342 (Molecular Probes, Life Technologies, #H-1399), Chicken anti-rabbit IgG secondary antibody Alexa Fluor 647 (Invitrogen, #A12443). Anti PECAM-1 for western blot, rabbit polyclonal IgG (Santa Cruz, #sc-8306), secondary swine anti-Rabbit-HRP antibody (DAKO, #P0399).

In vitro imaging

Live cells were imaged at 37° C and 5% CO2. Overlap was visualized by acquiring z stack images using fluorescence microscopy, Z-step size never exceeding 1 μ m. On the Leica SP8 machine with LAS X software (Leica Microsystems B.V.) images were acquired at 1024^*1024 resolution using the $40\times$ NA1.4 oil-immersion objective and fluorescence was detected using PMT and HyD detectors with suitable gain and AOBS filter settings. On the Zeiss LSM980 AiryScan2 machine (ZEISS) with ZEN software the $40\times$ NA1.4 oil-immersion objective was used for imaging at near-superresolution at $1.5\times$ Nyquist-sampling. On both microscopes, excitation lasers were 405nm for Hoechst and Alexa 405, 442nm for mTurqoise2, 488nm for mNeonGreen, 514nm for YFP, 561nm for mScarletl, 633nm for DiD, 633 nm and 671nm for respective Alexas.

Confocal overlap analysis

To quantify overlap, maximum projections of Z-stacks were obtained using ImageJ/FIJI. Before thresholding, noise was reduced using the despeckle tool and by using the 2D median filter with radius 2.0 pixels. Fluorescent vesicles were removed using the particle analysis tool or by hand. EC overlap width, length and area were quantified using ImageJ/FIJI measure tool.

Quantification of travel distance

PMN travel distances were quantified between first adhesion of the PMN on the monolayer and completed diapedesis. The travel start point was considered the PMN center of gravity upon adhesion. Then, the PMN center of mass was followed as it traveled the endothelium. The endpoint was considered the outer end of the overlap at the transmigration location.

In vivo imaging of TEM tunnels

Ischemia reperfusion injury (IR) was performed according to. 37 Briefly, AF-conjugated non-blocking anti-PECAM-1 mAb (4 μ g in 400 μ L PBS) was administered by intrascrotal (i.s.) injection for 2 h. Cremasteric IR injury was then induced in the exteriorized cremaster muscle of anesthetized mice by placing two non-crushing metal clamps (Interfocus, Schwartz Micro Serrefine) at the base of the exteriorized tissue (40 min). Subsequently, the clamps were removed to allow correct reperfusion of tissue and immunostained post-capillary venules (diameter: 20–40 μ m) of the cremaster muscle were imaged using an upright Leica TCS SP5, with argon and helium lasers (488, 561 and 633 nm excitation wavelengths), using water dipping 20×/1.0 objective lens. TEM events were recorded by taking serial Z-stacks for 1-2-h duration. A half-blood vessel was recorded, and the merged stack file/video represented an "enface" view of a selected post-capillary venule. Imaris software was used to apply an iso-surface of PECAM-1 to image the TEM tunnel.



QUANTIFICATION AND STATISTICAL ANALYSIS

Data was plotted and analyzed using GraphPad Prism 10.1.2. All experiments were performed at least triplicate, and the statistical parameters, including sample size and significance analysis, are detailed in the figure legends. Significance was determined using Unpaired, two-tailed Student's t test, Pearson correlation test, or Mann-Whitney U test. Quantitative data are presented as mean \pm S. E.M., and a *p*-value of <0.05 was considered statistically significant. All these parameters are given in the legends of the figures.